Delineation of ECG characteristic features using multiresolution wavelet analysis method

Article *in* Measurement · April 2012

1 author:

Rajarshi Gupta
University of Calcutta
37 PUBLICATIONS **129** CITATIONS

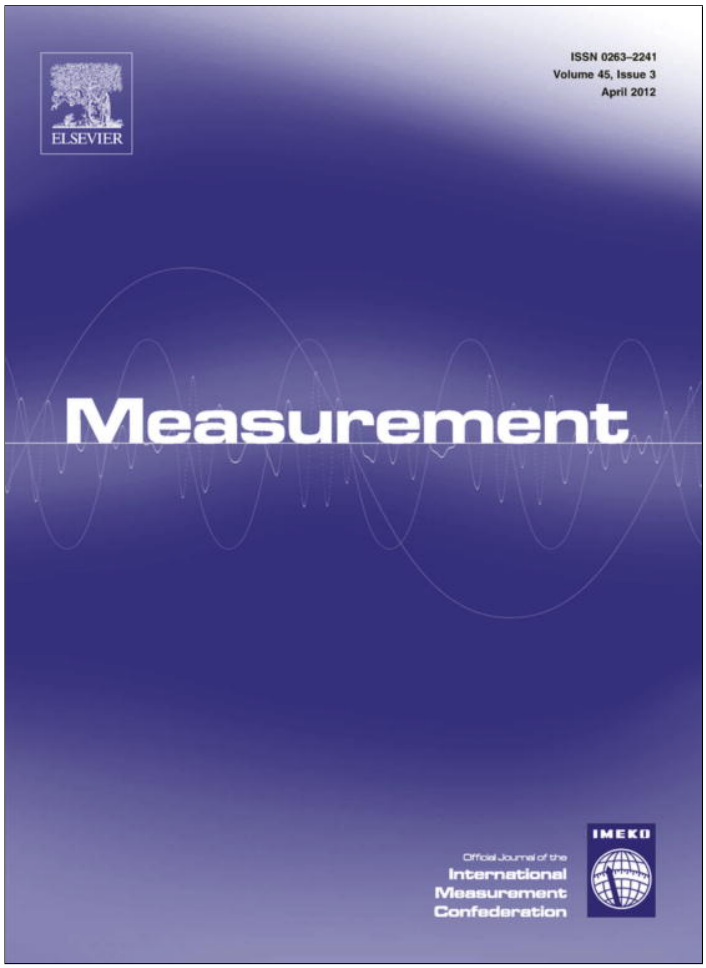

Measurement 45 (2012) 474–487

Contents lists available at SciVerse ScienceDirect

Measurement

journal homepage: www.elsevier.com/locate/measurement

Delineation of ECG characteristic features using multiresolution wavelet analysis method

S. Banerjee, R. Gupta, M. Mitra *

Department of Applied Physics, University of Calcutta, 92, APC Road, Calcutta 700 009, India

ARTICLE INFO

Article history:
Received 13 June 2011
Received in revised form 20 October 2011
Accepted 25 October 2011
Available online 9 November 2011

Keywords:
ECG fiducial points
Discrete wavelet transform
Multiresolution analysis
Denoising
Feature extraction

ABSTRACT

A discrete wavelet transform (DWT) based feature extraction technique in the *QT* segment of digitized electrocardiograph recordings is proposed. At first, the signal is denoised by decomposing it using DWT technique and discarding the coefficients corresponding to the noise components. A multiresolution approach along with an adaptive thresholding is used for the detection of R-peaks. Then Q, S peak, QRS onset and offset points are identified. Finally, the T wave is detected. By detecting the baseline of the ECG data, height of R, Q, S and T wave are calculated. For R-peak detection, proposed algorithm yields sensitivity and positive predictivity of 99.8% and 99.6% respectively with MIT BIH Arrhythmia database, 99.84% and 99.98% respectively with PTB diagnostic ECG database. For time plane features, an average coefficient of variation of 3.21 is obtained over 150 leads tested from PTB data, each with 10,000 samples.

1. Introduction

Electrocardiogram (ECG) is widely used for diagnosing many cardiac diseases, which are one of the prime causes of mortality all over the world. The origin of ECG is the electrical activation of heart muscle cell causing sequence of depolarization and repolarization of its membrane. The electrical pulses generated due to this electrical activation are propagated along the cell fiber and transmitted to adjoining cells. The result is generation of electrical impulses, which travels through the cardiac surface. These electrical impulses can be detected by surface electrodes, amplified and displayed as the ECG. From electrical point of view, the heart is situated at the center of the electrical field it generates. The intensity of its electric field diminishes with the distance from its origin. A 12-lead electrode system is used for ECG recording, exploring an overall view of the heart's electrical activity. ECG waveform consists of five different component waves, namely P, Q, R, S and T wave followed by a conditional U wave. A typical ECG beat is shown in Fig. 1. The durations and intervals of the constituent waves and amplitudes of the wave peaks reveal clinically significant information to the cardiologists for diagnosis [1].

Computerized processing of ECG for assisted diagnosis is an established area of biomedical research from long time. Performance of an automatic ECG analyzing system depends upon the reliable and accurate detection of the QRS complex and P and T waves along with the measurement of the *QT* segment. Detection and measurement of characteristic waves are related to diagnosis of various cardiac functions. For example, QRS detection is necessary to determine the heart rate and is used as reference for beat alignment. Likewise, ST segment elevation or depression is related to Myocardial Infarction.

The automatic delineation of the ECG is widely studied and algorithms are developed for QRS detection and wave detection [2–4]. A real time QRS detection algorithm, implemented in assembly language is developed by Pan and Tomkins [5]. Some early software based QRS detectors are presented [6–8]. ECG signal is normally corrupted with several noises, some of which are of physiological

* Corresponding author.
E-mail addresses: swatibanerjee29@yahoo.com (S. Banerjee), rgaphy@caluniv.ac.in (R. Gupta), mmitra@ieee.org (M. Mitra).

0263-2241/$ - see front matter © 2011 Elsevier Ltd. All rights reserved.
doi:10.1016/j.measurement.2011.10.025

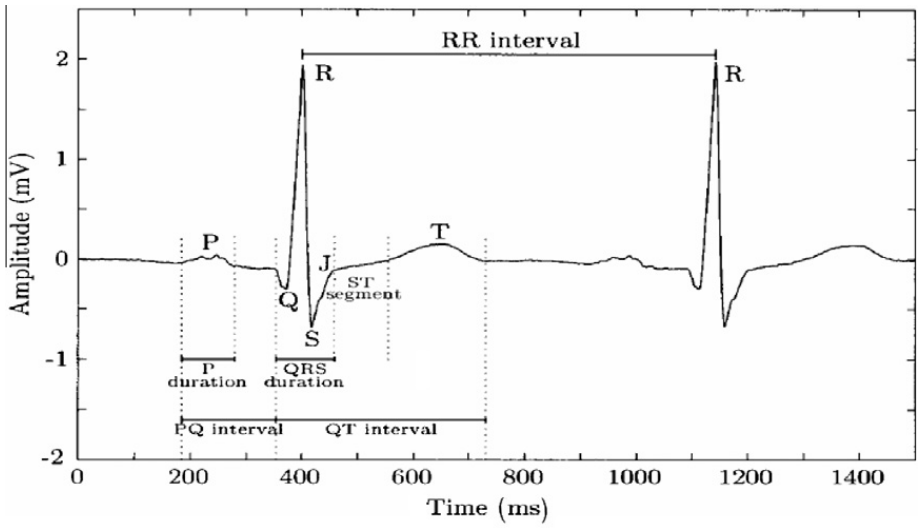

Fig. 1. ECG beat with marked characteristic points.

origin and others external. These are power line frequency interference, baseline drift, electrode contact noise, polarization noise, muscle noise, electrosurgical noise and the internal amplifier noise. So, denoising of the signal is a prerequisite to the accurate analysis. The noise sensitivity of nine different QRS complex detectors analyzed by Friesen et al. [8].

Frequently, for computerized determination of wave peaks and corresponding onset and offset points, QRS detection is the starting point. QRS location is represented by R peak index, or QS peak index in case of positive R absent. In time domain processing of samples, the individual fiducial points are determined with respect to the corresponding QRS index of the same beat by window search of appropriate width using magnitude and slope based criteria. Since ECG morphology varies among different age groups, communities and subcontinents, in addition to numerous types of cardiac diseases, there exists no golden rule for detection of the wave boundaries accurately. In an attempt to develop more accurate algorithms for extraction of features different approaches are used. Some algorithms are based on mathematical models [9,10]. A simple, mathematical based method along with the concept of data structure is used to obtain the complex [11]. A new mathematical based QRS detector using CWT is explored in [30]. Some other approaches like matched filters [12], ECG slope criteria [13], second order derivatives [15], wavelet transforms [16], [17] are also studied. In [16], a multi-scale QRS detector including a method for monophasic P and T waves was proposed. Method based on evolutionary optimization process [18] is reported for wave delineation. ECG beats are classified by neuro-fuzzy networks where predefined feature vectors are used [19]. A rule mining based method is developed [20], where ischemic beats are identified by extraction of features followed by feature discretization and rule mining. ECG features was also extracted using linear predictive coding in [21]. Natalia et al. [29] has analyzed first derivative based QRS detection algorithm. A wavelet based soft decision techniques is proposed for identification of patients with cognitive heart failure [32], it uses power spectral density and soft computing techniques for the purpose. Feature measurement of ECG beats based on statistical classifier is explored in [33]. Integration of independent component analysis and neural networks for ECG beat classification is also an effective technique for classification of ECG beats [34]. A method of analysis of Myocardial Infarction is explored using discrete wavelet transform in [35].

The wavelet transform (WT) provides a description of a signal, decomposing it at different time–frequency resolution. WT is a well suited tool for analysis of non-stationary signals like ECG. The different wave components of ECG having separate frequencies, becomes clearly visible when subjected to multiresolution analysis. Moreover the various noise levels, which appear at different frequency bands and their contribution towards distortion of the signal, can be clearly identified.

In this paper, a discrete wavelet transform (DWT) based ECG feature extraction technique in the *QT* region is proposed. The developed algorithm extracts various clinical signatures from the ECG data by determining the fiducial points from a single lead data. Some of the extracted time-plane features are QRS width, *QT* interval, R height, T height. The algorithm validated using ECG records from PTB diagnostic ECG database (ptb-db) and MIT-BIH arrhythmia database (mit-db) under Physionet [23,31] are used. After decomposing the signal using DWT, well localized frequency domain features are obtained at different levels of decomposition. QRS complex and T wave frequency bands are identified along with the frequency levels for different noises. The signal is denoisied by discarding those frequency bands corresponding to noise levels. A multiresolution approach along with thresholding is used for the detection of R-peaks in each cardiac beat. Hence, the heart rate is calculated. Then other fiducial points (Q and S) are detected by differentiation and slope criteria based search. QRS onset and offset points are detected. Finally, the T wave peak is detected and *QT* interval

is measured. Baseline is also detected in the *TP* segment and height of R, Q, S and T waves are calculated.

2. Materials and methods

2.1. Wavelet theory

Wavelet transform is a linear transform, which decomposes a signal into components that appears at different scales (or resolution). It is a decomposition of signal using a combination of a set of basis functions, obtained by means of dialation (scaling) and translation of a single prototype wavelet. The greater the scale factor, wider is the basis function and consequently, the corresponding components give the low frequency component of the signal and vice versa. In this way the temporal resolution is higher at high frequencies than at low frequencies achieving the property that the analysis window comprises the same number of periods for any central frequency.

2.1.1. Multiresolution wavelet analysis for feature extraction

Time localization of spectral components can be obtained by multiresolution wavelet analysis, which provides the time–frequency representation of the signal. Among many time–frequency representations, the DWT, using a dyadic scale is perhaps the most efficient one due to its many unique properties and its ability to solve a diverse set of problems including data compression, biomedical signal analysis, feature extraction, noise suppression and many more all with a modest amount of computational expense.

The DWT analyses the signal at different resolution (hence, multiresolution) through the decomposition of the signal into several successive frequency bands. The DWT utilizes two set of functions $\varphi(t)$ and $\psi(t)$, each associated with the low pass and the high pass filters respectively [22]. These functions have a property that they can be obtained as the weighted sum of the scaled (dilated) and shifted version of the scaling function itself:

$$\phi(t) = \sum_n h[n]\phi(2t - n) \tag{1}$$

$$\psi(t) = \sum_n g[n]\phi(2t - n) \tag{2}$$

Here, $h[n]$ and $g[n]$ are the half band low pass filter and high pass filter respectively.Conversely, a scaling function $\varphi_{j,k}(t)$ or wavelet function $\psi_{j,k}(t)$ that is discretized at scale j and translation k can be obtained from the original (prototype) function $\varphi(t) = \varphi_{0,0}(t)$ or $\psi(t) = \psi_{0,0}(t)$.

$$\psi_{j,k}(t) = 2(^{-j/2})\psi(2^{-j}t - k) \tag{3}$$

$$\phi_{j,k}(t) = 2(^{-j/2})\phi(2^{-j}t - k) \tag{4}$$

where j controls the dilation or translation and k denotes the position of the wavelet function.

Different scale and translation of these functions allows one to obtain different frequency and time localization of the signal. Decomposition of the signal into different frequency bands is therefore accomplished by successive low pass and high pass filtering of the time domain signal. The original time domain signal $x(t)$ sampled at 1000 samples/s forms a discrete time signal $x[n]$, which is first passed through a half-band high pass filter $g[n]$, and a low pass filter $h[n]$ along with down sampling by a factor of 2.

Filtering followed by sub-sampling constitutes one level of decomposition, and it can be expressed as follows:

$$D1[k] = y_{\text{high}}[k] = \sum_n x[n] \cdot g[2k - n] \tag{5}$$

$$A1[k] = y_{\text{low}}[k] = \sum_n x[n] \cdot h[2k - n] \tag{6}$$

where $y_{\text{high}}[k]$ and $y_{\text{low}}[k]$ are the outputs of the high pass and low pass filters, respectively. The DWT decomposition tree for a signal with 1 kHz of sampling frequency is shown in Fig. 2. The detail coefficients are designated as D_n and approximation coefficients as A_n, where $n = 1$–10

In the ptb-db data files, sampling frequency of the ECG data is 1 kHz. The DWT decomposition of the signal using

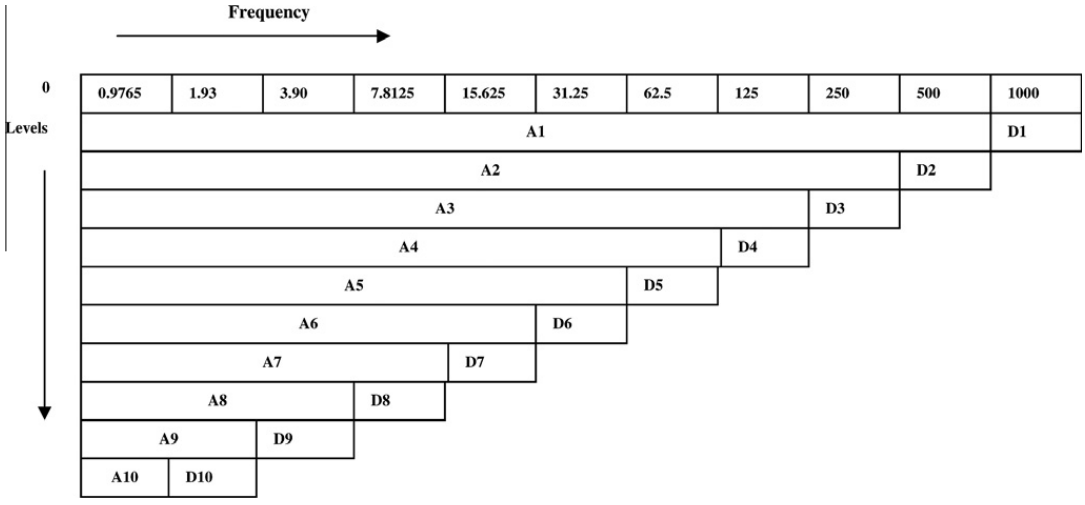

Fig. 2. DWT decomposition structure.

any particular wavelet function is actually the segregation of the signal in different frequency bands and hence extracting the time–frequency details. Selecting a wavelet function, which closely matches to the morphology of signal under investigation is of great importance in wavelet based application [24]. Daubechie's wavelet families are similar to the shape of the QRS and hence db6, having close similarity with QRS morphology and having the energy concentration at low frequencies, is being selected as the mother wavelet for the present analysis. The selection of the scale (frequency band) is based on sampling frequency of the current data file along with a prior knowledge of the clinical bandwidth of the signal and various noise levels. The proposed algorithm is adaptive to other sampling frequencies and prior to any analysis, takes the sampling frequency as input and divides it in a dyadic scale, and

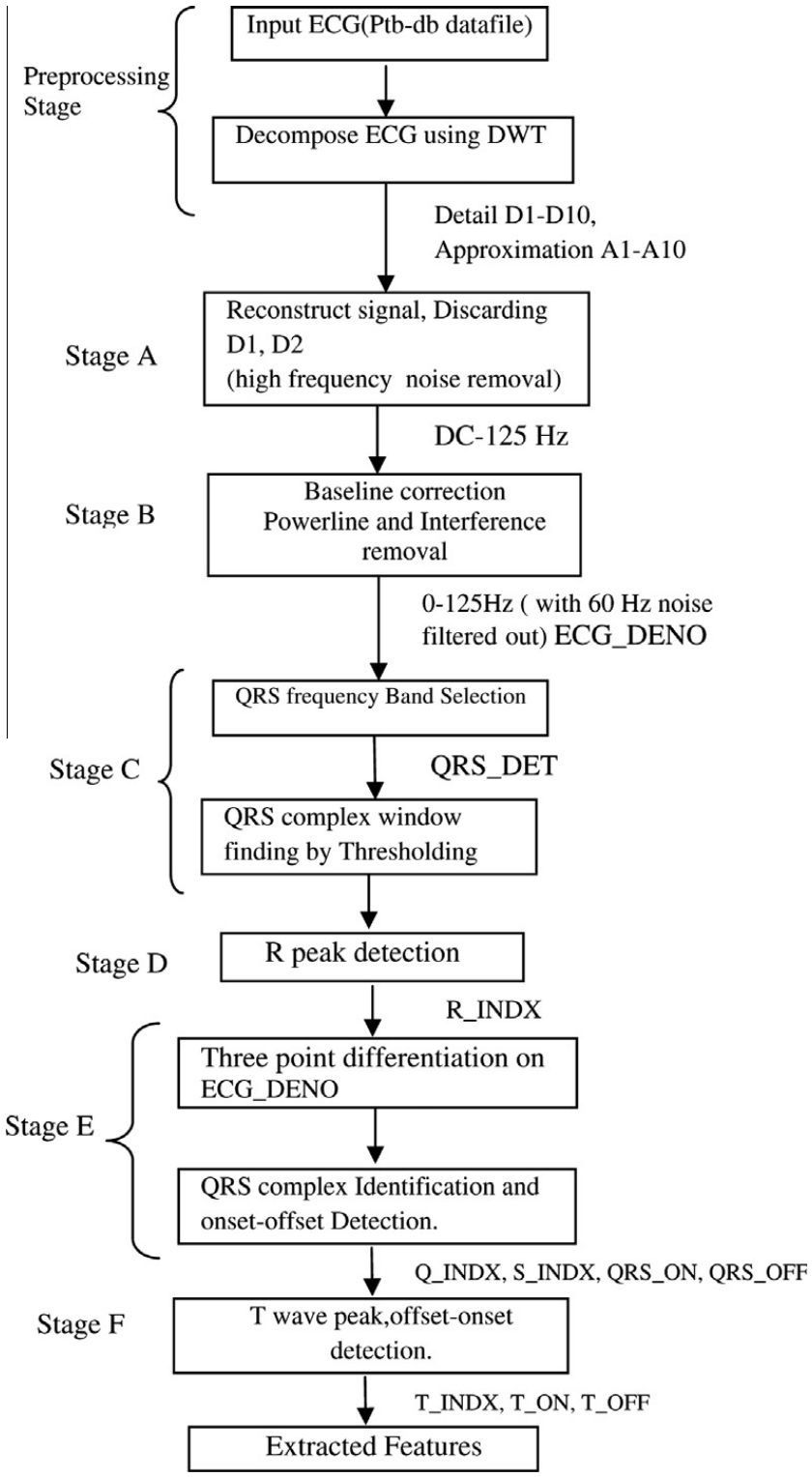

Fig. 3. Block schematic of the processing stages.

hence, selects the frequency band of relevant interest as the noise frequencies and ECG bandwidth is already known [8]. For example this range will lie in *A*2 if the sampling frequency is 360 Hz. Another viable method is to resample this frequency to 1 kHz which is not considered here. The block schematic presentation of the proposed algorithm illustrating the stages is shown in Fig. 3. The preprocessing stage consists of the lead selection and DWT decomposition of the lead data. The signal is denoised in stages A and B by identification of noisy frequency bands and hence rejecting corresponding coefficients. The output of stage B is an array ECG_DENO, which contains the noise free signal. Stage C represents the QRS frequency band selection from the detail coefficients *D*4 and *D*5, and generation of an array QRS_DET, which contains QRS information. Stage D describes processing of QRS complex window to detect R peaks. Stage E deals with denoised array ECG_DENO by differentiation and detection of fiducial points Q onset, S offset, Q and S peak. The final stage F detects T peak, its offset and onset. Hence, the characteristic signatures from the ECG data are computed. The following section illustrates the processing stages A–F.

2.2. Denoising the signal

In this stage the noise frequency identification and their elimination is carried out in two basic steps, viz, (A) high frequency noise removal, (B) baseline wander correction and power line interference removal.

2.2.1. High frequency noise removal

Electrosurgical noise and muscle contraction noise are high frequency noise. Electrosurgical noise completely destroys the ECG and without its removal an accurate feature extraction cannot be accomplished. The frequency content of this noise is 100 kHz–10 MHz. Since the sampling frequency of the data is 1 kHz an aliased version gets added to the ECG. The muscle contraction noise has a frequency range from dc-10 kHz. These two noises are eliminated by discarding the detail coefficients *D*1, *D*2. After removal of these noises the remaining ECG signal ranges from 0 to 125 Hz.

2.2.2. Baseline correction and power line interference removal

The drift of the baseline is caused due to respiration and is likely to be as a nearly sinusoidal component and the frequency of respiration gets added to the ECG during its acquisition. The baseline variation frequency is 0.15–0.8 Hz. Motion artifacts are transient baseline changes caused by change in the electrode skin impedance with electrode motion. The baseline disturbances caused by motion artifact can be assumed as a signal resembling one cycle of a sine wave and is within the frequency range of baseline drift. These two type of noises stated above can be eliminated by removal of the lowest frequency component, after decomposition of the ECG signal As shown in Fig. 4, coefficient *A*10 contains this frequency along with the DC component of the ECG. Discarding *A*10 frequency band and reconstructing the signal eliminates these two noises.

Power line interference contains a 60 Hz noise intertwined with the ECG. In India the power line frequency is 50 Hz. In this work, ptb-db data files under Physionet are used for evaluation of the proposed method, where the power line frequency is 60 Hz. Electrode contact noise is transient interference caused by loss of contact caused by the electrode and skin. During this time short duration power line interference corrupts the ECG. These two noises

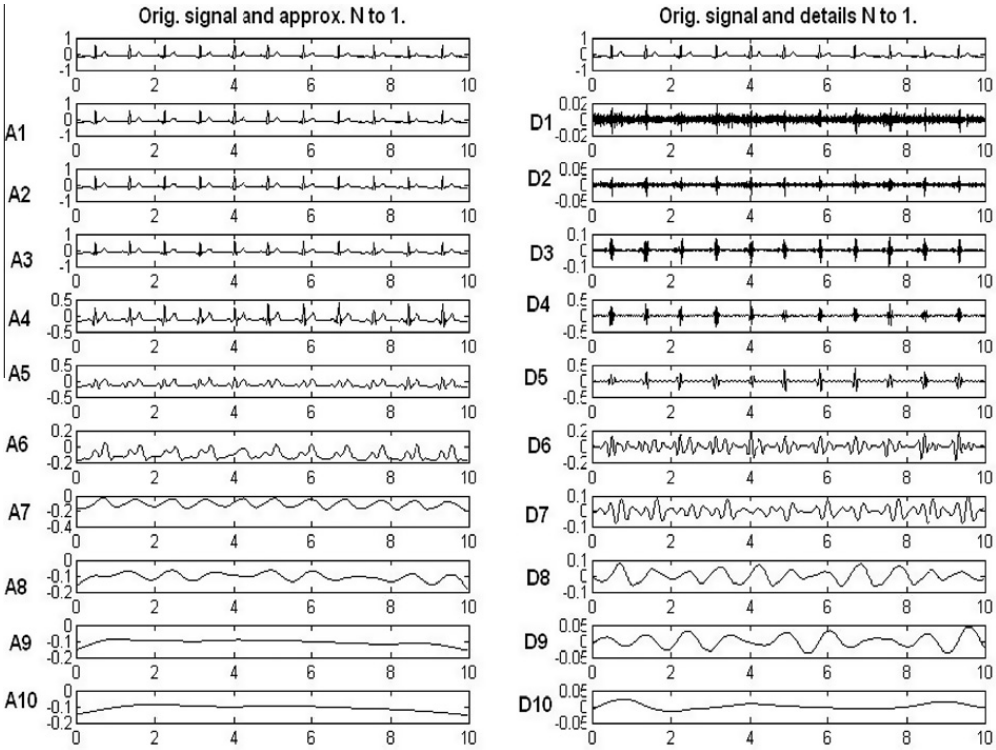

Fig. 4. The DWT decomposition and corresponding details and approximations.

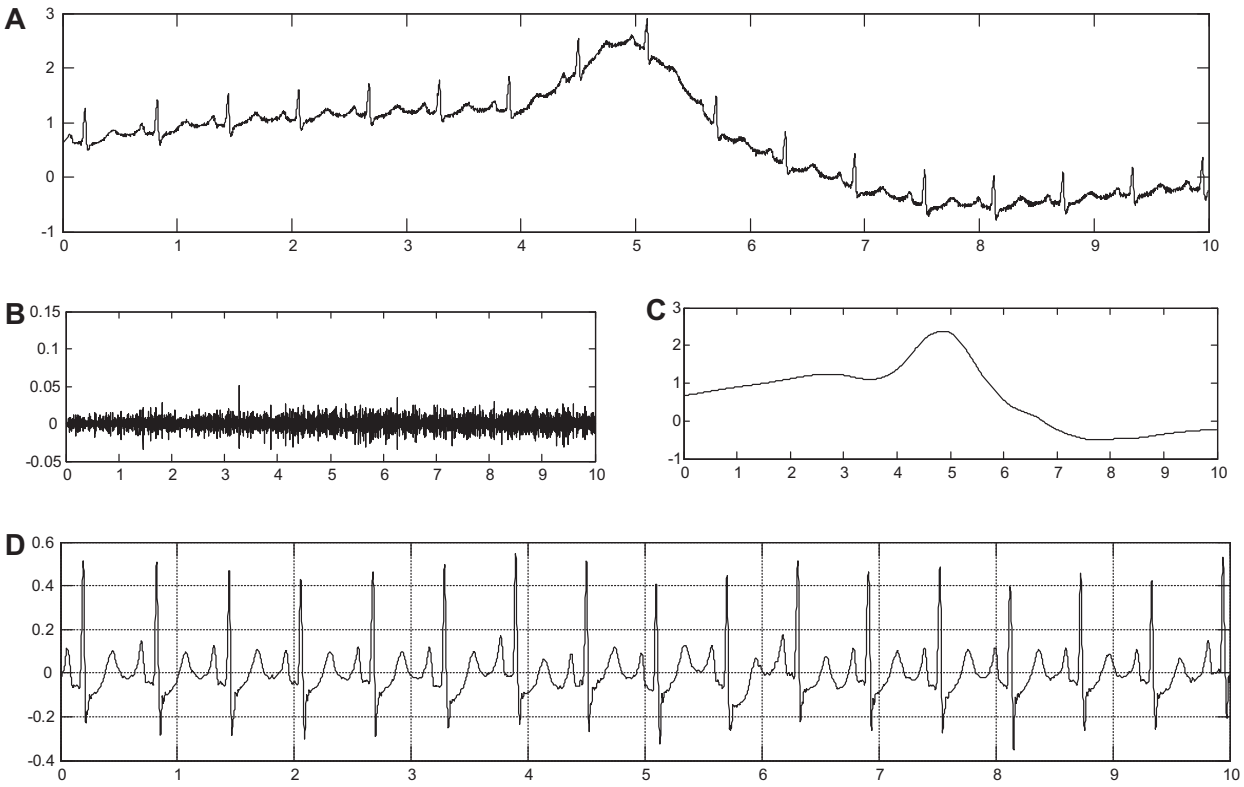

Fig. 5. A. Original ECG signal, B. High Frequency Noise, C. Low Frequency noise, D. Denoised and Baseline Corrected ECG signal.

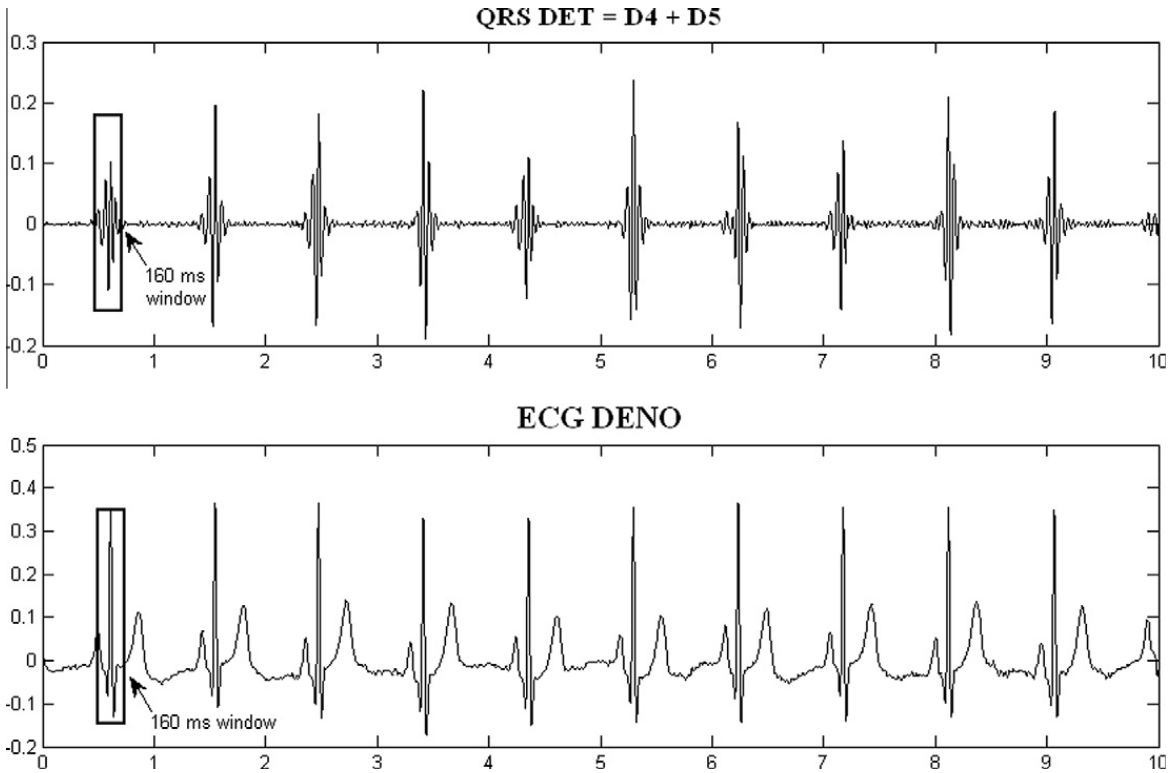

Fig. 6. R peaks of QRS complex located in original signal from QRS_DET.

can be eliminated by the dyadic scale DWT technique by identification of the frequency band containing the frequency range of 59.5–60.5 Hz. The signal output from stage B is in the frequency band 0–125 Hz in Fig. 3. On further decomposing the signal, the low pass component ($A5$) will have 0–62.5 Hz and high pass component ($D5$) will have 62.5–125 Hz. As shown in Fig. 2 the noise is in the low pass component, so it is decomposed. The next

level decomposition yields 0–32.25 Hz signal component (say $D5_a$) and 32.5–62.5 Hz signal (say $D5_b$). Now the high pass component $D5_b$ (containing the 60 Hz noise) is decomposed. The signal component $D5_b$ containing the noise frequency is continuously decomposed until the frequency band of 59.5–60.5 Hz is obtained. This component is rejected and the signal from the rest of the decomposed components is reconstructed. This reconstructed signal is the noise free signal, taken in an array named ECG_DENO. Fig. 5 shows a typical representation of original noisy signal, extracted high and low frequency noises and noise-free signal. This is shown in stage B of Fig. 3.

2.3. QRS complex band selection and finding the QRS window by thresholding

In this stage the objective is to find out the QRS region from the detail coefficients of the DWT decomposition and mapping of this zone in the denoised array ECG_DENO. From Fig. 4, it is observed that the QRS complex regions are more prominent in details at scale $D3$–$D5$, among which the most of the energy of the QRS complex is concentrated [14,18]. For signals with high noise content the components $D4$ and $D5$ are to be considered. An array QRS_DET is formed by addition of components $D4$ and $D5$. The QRS complexes are clearly visible from Fig. 6, which shows QRS_DET plot against ECG_DENO. To find out the QRS complexes from QRS_DET, an empirically determined threshold value is set which is equal to the 15% of the mean amplitude value of QRS_DET array. To detect the R peaks accurately, the indexes which exceed the threshold level are marked in the QRS_DET array. The region of the QRS complex starts from the first point where the absolute QRS_DET value becomes greater than the threshold. Since the maximum width of the QRS complex for any patient is not more than 160 ms [1], a fixed window of same width is searched in QRS_DET to detect the indexes where the threshold condition is satisfied. Between two consecutive searches a blanking period of 200 ms is offered [5]. The rule used in stage C is:

Threshold = 15% of (mean amplitude of absolute QRS_DET).

Algorithm steps for QRS complex region finding is given as:

QRS_DET = $D4 + D5$

SET: Threshold = 15% of mean amplitude of absolute QRS_DET

1. $i = 1$; $k = 1$;
2. if QRS_DET(i) > Threshold, go to step 5;
3. $i = i + 1$;
4. go to step 1;
5. QRS region $(k) = x + 160$;
6. $k = k + 1$; $i = i + 200$;
7. go to step 1.

A new array QRS_START is formed which contains starting index of all QRS complex.

2.4. R peak detection (Q or S in case of QS complex)

The R (Q or S) peaks are the maximum (minimum) amplitude values within the QRS windows, set over ECG_DENO. In stage D, mapping each of the QRS starting index to the denoised signal ECG_DENO, the actual R peaks (Q or S peak) can be obtained by searching the local maximum (minimum) value within each QRS_START : QRS_START + 160 ms window. The amplitude of each R – index is again checked from ECG_DENO. If this is positive (negative), an R peak (an elongated or pathological Q or S) is identified. So, by this method all the peaks of the QRS complex are identified. The rule for R peak detection is given as:

- Peak = absolute_maximum(QRS region).
- IF Peak is POSITIVE.
- THEN ‘R peak detected’.
- ELSEIF Peak is NEGATIVE.
- THEN ‘Q or S is detected’.

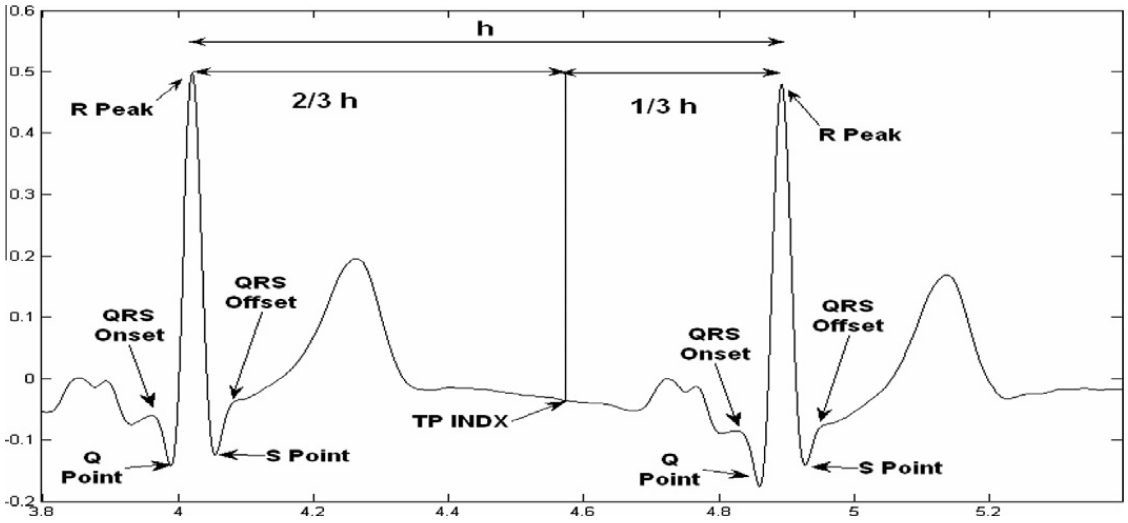

Fig. 7. Region ratio between T offset of current beat and P onset of next beat.

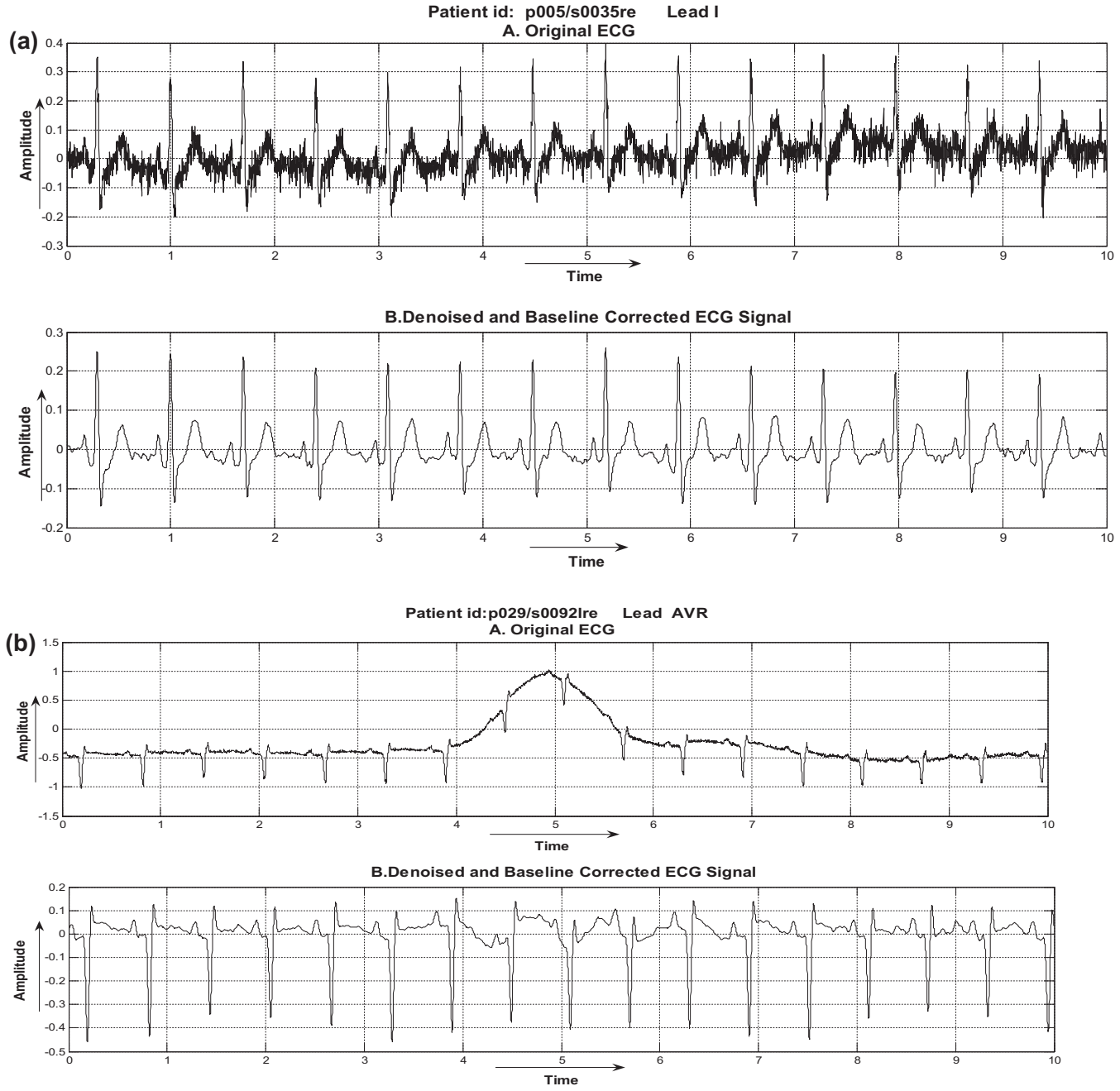

Fig. 8. Denoising of ECG signal. (a) Denoising from high frequency noise and (b) denoising from baseline modulation.

Table 1
Beat detection on ptb-db.

Patient ID and record no. from Physionet	Total no. of beats	Detected beats	*TP*	*FN*	*FP*	S_e (%)	*P*+ (%)
P024/s0083lre	7692	7662	7662	30	0	99.6	100
P117/s0291lre	8040	8040	8040	0	0	100	100
P007/s008lre	9360	9341	9339	21	2	99.8	100
P041/s0130lre	7680	7689	7680	0	9	100	99.8
P027/s0089lre	10,080	10,060	10,058	22	6	99.8	99.9
Total	42,852	42,832	42,779	73	8	99.84	99.92

All the R (Q or S) indexes are stored in an array R_INDX. The heart rate can be computed from the average R-R interval. For accurate detection of fiducial points in the following stages a 'feature detection zone' is selected, where no peak is wrongly detected (either 'false positive' and 'false negative'). A threshold limit (THS_LMT) is

Table 2
Beat detection on MIT-BIH Arrhythmia database.

Patient ID from Physionet	Total no. of beats	Detected beats	*TP*	*FN*	*FP*	S_e (%)	*P*+ (%)
100	2273	2273	2273	0	0	100	100
101	1865	1868	1865	6	9	99.6	99.5
102	2188	2188	2188	0	0	100	100
103	2084	2084	2084	0	0	100	100
104	2230	2230	2230	0	0	100	100
105	2572	2569	2558	14	11	99.4	99.5
106	2027	2027	2027	0	0	100	100
107	2137	2137	2137	0	0	100	100
108	1764	1764	1764	0	0	100	100
Total	19,140	19,140	19,126	20	20	99.6	99.5

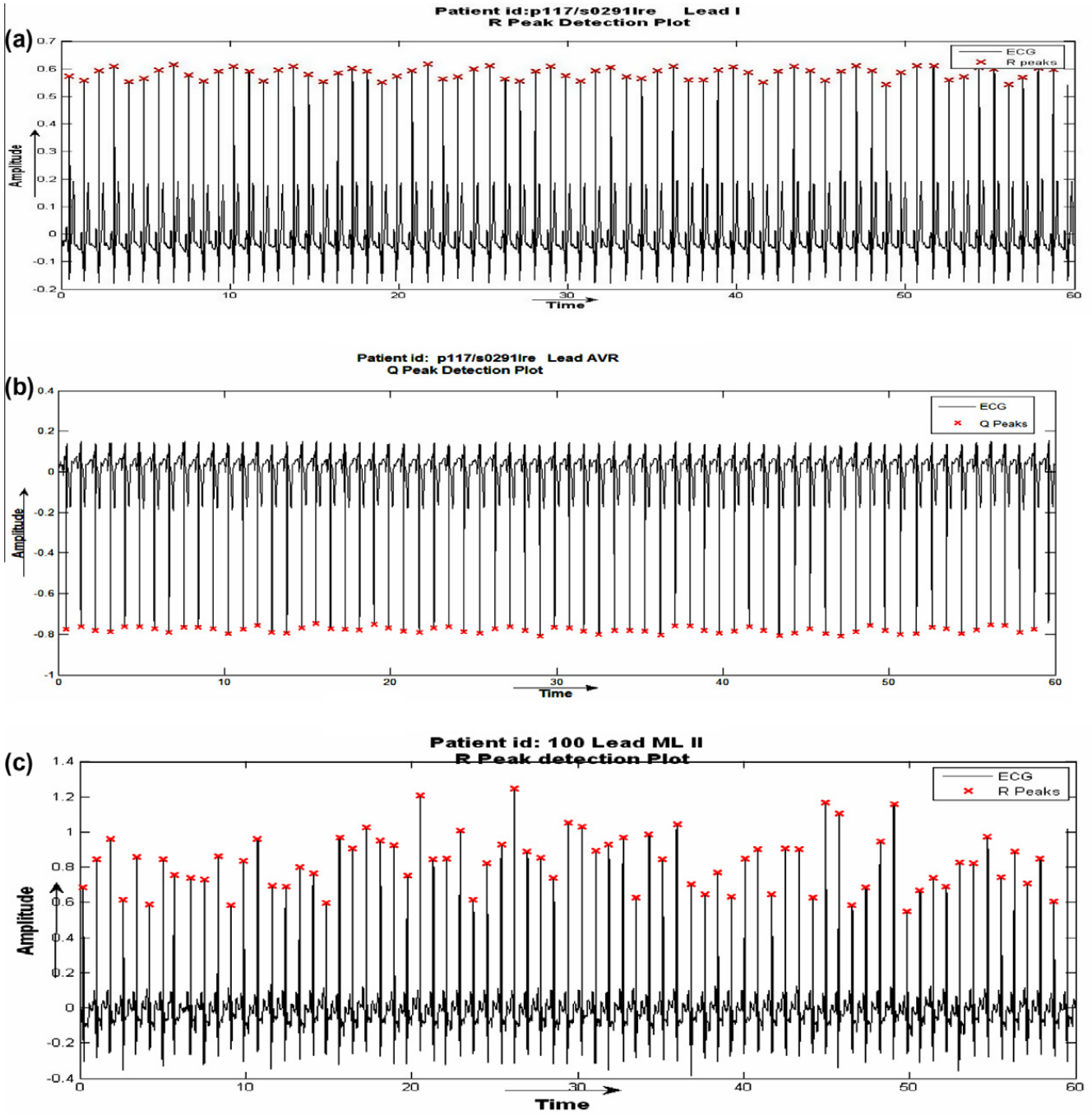

Fig. 9. Detection of R-peaks using 60 s Physionet data; (a) using ptb-db data (positive R peak); (b) using ptb-db data (pathological Q peak); (c) using mit-db data.

computed from the average *R–R* interval and is set to select the feature extraction zone, given by the following equation:

$$\text{THS\_LMT} = \text{R—R} \pm 20 \text{ ms}$$

The rule for selecting proper feature extraction zone is:

- SET: THS_LMT = Average *R–R* interval ± 20 ms.
- IF *R–R* interval > THS_LMT.
- THEN 'False Negative'.
- ELSEIF *R–R* interval < THS_LMT.
- THEN 'False Positive'.
- ELSE *R–R* interval within THS_LMT.
- THEN 'Feature Extraction Zone Selected'.

2.5. Q and S point, with QRS onset and offset detection

Once the R peak is detected accurately, the Q and S points are detected in stage E to find the complete QRS complex. To detect the position of Q (and S) points, search is initiated from an R peak towards left (Right) within a window of R_INDX: R_INDX-80 (for S, R_INDX: R_INDX + 80) to check the slope sign inversion. For each point on ECG_DENO, the slope is computed by three point differentiation using the formula:

$$f'(x) = \frac{f(x+h) - f(x-h)}{2h} \tag{7}$$

where h is the time division.

In case a detected peak is of negative amplitude, the algorithm decides whether it is an elongated (pathological) Q or S wave depending on its nearby vicinity from the left or right side of the window and same technique is adopted for finding the other fiducial points. The found peaks are taken in an array Q_INDX and R_INDX and S_INDX. Hence, all the Q, R, S peaks are marked.

Ordinarily, the Q and S waves are high frequency and low amplitude components. The corresponding onset and offset values are the points having nearly zero or minimum slope region before the Q and after the S wave. After the detection of the R peak, the corresponding onset (offset) of the QRS complex is determined from Q peak index Q_INDX (S peak index S_INDX) by a 40 ms window search towards the upside (downside) along the ECG_DENO array. The position of minimum slope in the region of Q_INDX: Q_INDX-30 (for S Offset S_INDX:S_INDX + 30) is detected and taken as QRS onset (QRS Offset). For S-offset, a 20% relaxation is allowed to meet the slope criteria. The Q onset indexes are taken in an array QRS_ON and S-offset indexes in QRS_OFF. If the amplitude of the Q wave peak is closer to

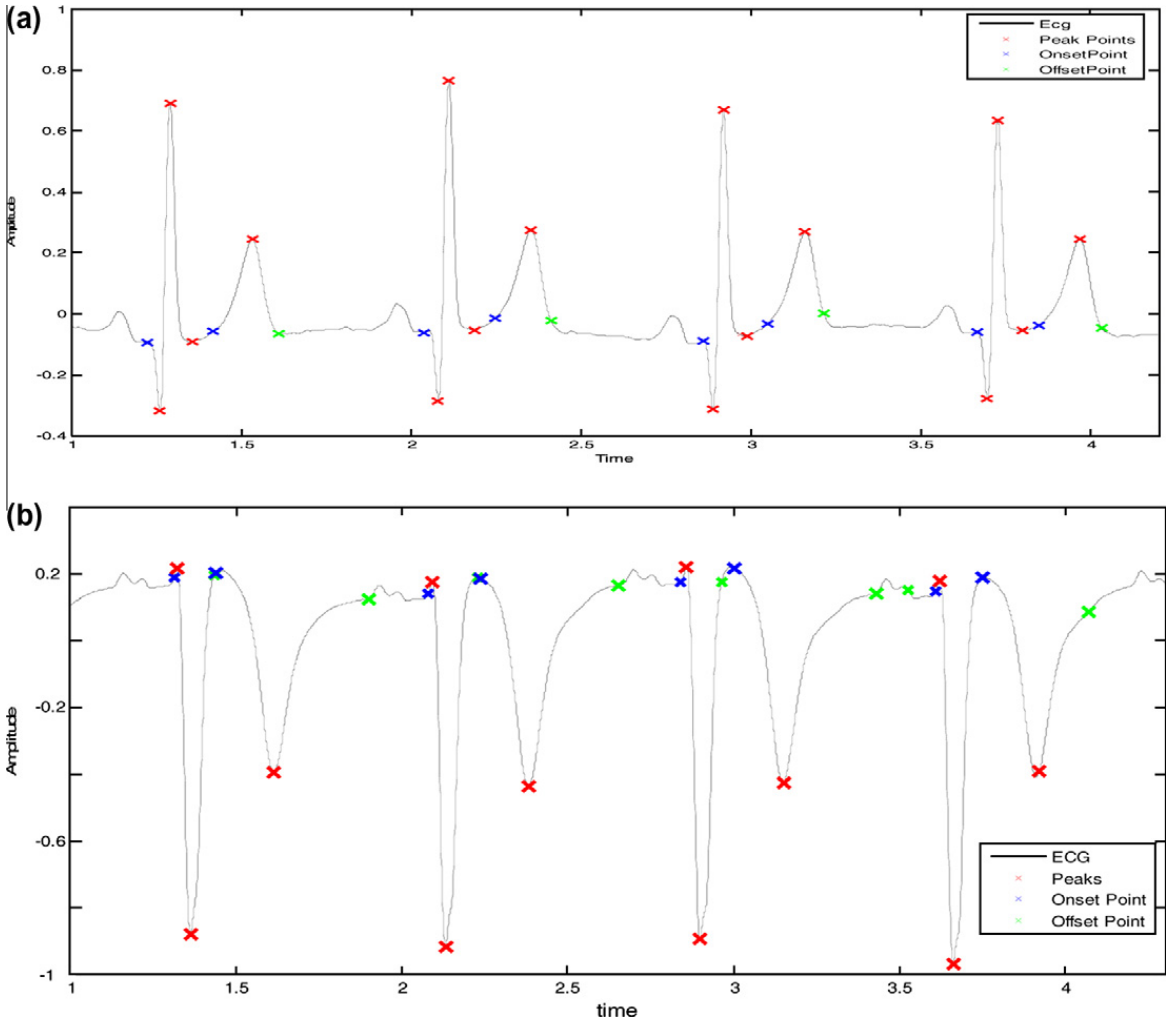

Fig. 10. Fiducial point determination from ptb-db data; (a) using normal data (Normal Lead V2) and (b) abnormal data (Anteroseptal MI Lead V2).

the onset, then there is no significant Q wave in the ECG and similar is the case for S wave and offset.

The rule for detecting the Q and S points:

- Q_INDX = Point of Slope sign inversion (R_INDX: R_INDX-80).
- S_INDX = Point of Slope sign inversion (R_INDX: R_INDX + 80).
- The rule for detecting the QRS onset is:
- QRS_ ON = MIN_SLOPE (Q_INDX: Q_INDX- 40).
- The rule for detecting the QRS offset is:
- SET: SLOPE_S = the slope of S_INDX: S_INDX + 40.
- SLOPE_TH = 0.2 × (Maximum slope in S_INDX: S_INDX + 40).
- IF SLOPE_S (k) > = SLOPE_TH.
- THEN QRS_ OFF detected.

2.6. T wave detection

After the offset of S wave is identified, the search for T wave is initiated. The interval between two consecutive QRS_OFF and QRS_ON is calculated, and this is divided in a ratio of 2:1, which is demarcated by TP_INDX. Usually, the T peak of the current beat is expected occur in the first (left w.r.t TP_INDX) zone and P wave of the following beat in the next (right w.r.t TP_INDX) zones. This is depicted in Fig. 7. The T-search zone is defined as: QRS_OFF (k): TP_INDX. The point with absolute maximum value in this zone is considered as T-peak. Here, k indicates current beat index. All such indexes are taken in an array T_INDX. Similarly, P peak is found in the zone TP_INDX:QRS_ON ($k + 1$), and all indexes are taken in an array P_INDX. Now the window of T wave is estimated and the T wave detection method is applied within this window.The rule for detecting the T wave:

- Divide the QRS_OFF (k): QRS_ON ($k + 1$) interval in a ratio of 2:1 = T-zone: P-zone.
- T wave detection region estimated.
- Find absolute maximum amplitude value in this zone.
- IF T peak is POSITIVE.
- THEN 'T Upright'.
- ELSEIF T peak is NEGATIVE.
- THEN 'T Inverted'.

2.7. Baseline detection

Normally, the *TP* segment (region between T offset of current beat and P onset of next beat) is regarded as the baseline or the iso-electric line of the ECG signal [1]. The region after the end of T wave of the current beat and before the start of P wave of the following beat is *TP* section. It also marks the end of one cardiac cycle. In the *TP* segment, the index with minimum absolute slope within a window of 25 samples is considered as the baseline point. The voltage at this index is nearly zero.

3. Testing and result

The algorithm is validated with arbitrarily chosen ECG data from Physikalisch-Technische Bundesanstalt diagnostic ECG database (ptb-db) of Physionet [23], which contains 549 records from 290 subjects with 52 healthy controls and 148 Myocardiac infarction patients. This algorithm is tested on 12-lead ECG records, each of 10 min duration. Since ptb-db database contains 12-lead signal, it corresponds to 12 different patterns, each having different characteristic features. The R peak detection method is tested on the MIT BIH Arrhythmia ECG database. This database is developed and distributed since 1979 from laboratories at Boston's Beth Israel Hospital (BIH) and MIT for different research activity for arrhythmia analysis and related subjects. The database consists of 48 half-hour recordings for a total of 24 h of ECG data. Each record contains data for two channels.

The denoising of the signal and baseline correction as explained in stage A and stage B are shown in Fig. 8a and b respectively. Fig. 9a, b shows the R peak detection from

Table 3
Time features.

Patient ID and record no. from Physionet	Lead	QRS width (s)		*QT* segment length (s)				QT_c (s)	*R–R* interval (s)		
		Mean	SD	C.V (%)	Mean	S.D	C.V(%)		Mean	S.D	C.V (%)
P024/s0083lre (antero-septal MI)	V1	0.0994	.0055	5.6	0.338	0.0024	7.2	0.390	0.749	.0068	0.92
	V2	0.0986	.0059	5.9	0.394	.0027	6.9	0.45	0.746	.0066	0.89
	V3	0.0832	.0021	2.6	0.356	.0020	5.7	0.41	0.751	.0076	1.02
	V4	0.0790	.0026	3.4	0.401	.0024	6.1	0.46	0.740	.0067	0.91
P013/s0045lre (antero-septal MI)	V1	0.093	.0066	7.1	0.198	.0221	11.2	0.236	0.703	.0025	0.36
	V2	0.085	.0052	6.2	0.291	.0285	9.8	0.34	0.703	.0022	0.32
	V3	0.089	.0055	6.5	0.295	.028	9.9	0.35	0.705	.0021	0.30
	V4	0.085	.0053	6.3	0.285	.0285	10.1	0.34	0.701	.0022	0.32
P117/s0291lre (normal)	V1	0.101	.0041	4.1	0.332	.0169	5.1	0.35	0.880	.0043	0.49
	V2	0.096	.0044	4.6	0.356	.018	5.3	0.37	0.884	.0042	0.48
	V3	0.081	.0039	4.9	0.341	.016	4.9	0.362	0.884	.0039	0.45
	V4	0.094	.0039	4.2	0.355	.018	5.1	0.377	0.883	.0039	0.45
P104/s0306lre (normal)	V1	0.086	.0031	3.7	0.267	.011	4.2	0.281	0.901	.0060	0.67
	V2	0.093	.0028	3.1	0.263	.011	4.2	0.275	0.9111	.0061	0.67
	V3	0.1089	.0033	3.1	0.328	.014	4.3	0.34	0.91	.0058	0.64
	V4	0.098	.0028	2.9	0.409	.016	4.1	0.45	0.901	.005	0.65

ptb-db and Fig. 9c from mit-db data respectively. For better visibility only a 1 min plot is shown.

The sensitivity and positive predictivity are the performance analysis metric of any QRS detection method and are expressed by the following equations:

$$\text{Sensitivity}(S_e) = \frac{TP}{TP + FN} \tag{8}$$

$$\text{Positive Predictivity}(P+) = \frac{TP}{TP + FP} \tag{9}$$

where TP = True positive (correct detection of R-peak), FN = False negative (undetected R peaks), FP = False Positive (misdetections).

The partial beat detection results are tabulated in the Table 1 for ptb-db and Table 2 for mit-db, showing the sensitivity figures. An average detection rate of 99.84% is found over 150 leads tested from ptb-db. For the mit-db the figure is 99.6% over 60 leads.

Once the R peak (or the pathological Q or S) is correctly detected as the maximum amplitude peak, the associated Q and S waves (or R and S/Q and R wave) can be accurately determined. The detection of ECG fiducial points for one normal and one abnormal (anteroseptal-MI) data from ptb-db are shown in Fig. 10a and b respectively.

The heights of various waves are calculated as:

- Q height = QRS-onset amplitude – Q-peak amplitude.
- S height = QRS offset amplitude - S amplitude.
- R height = R amplitude – baseline from *TP* region.
- T height = T peak amplitude – baseline from *TP* region.

The time-plane features in *QT* segment are determined as:

- *R–R* interval = Distance between two consecutive R peaks.
- QRS width = QRS onset – QRS offset.
- *QT* interval = QRS onset – T offset.
- The *QT* interval is corrected for what it will be theoretically be at a rate of 60 beats per minute, giving a normalized value.

$$\text{So,} \quad QTc = \frac{QT}{\sqrt{R\text{–}R}} \tag{10}$$

The feature extraction performance analysis metric which are used for the validation of the test results are stated below. The mean of all the measurement of individual characteristic points, their standard deviations along with the coefficient of variation are calculated.Here, x_i = ith beat, n = number of beats.

$$Mean = \frac{1}{n}\sum x_i \tag{11}$$

$$Standard\ Deviation(S.D) = \sqrt{\frac{\sum (x_i - mean)^2}{n}} \tag{12}$$

$$Coefficient\ Of\ Variation(COV) = \frac{S.D}{Mean} \times 100 \tag{13}$$

The standard deviation (S.D) and Coefficient of variation (COV) is measured for the extracted features. SD measures the absolute dispersion or variability of a distribution. It

Table 4
Amplitude features.

Patient ID and record No. from Physionet	Lead	Q height			R height			S height			T height		
		Mean	S.D	C.V (%)	Mean	S.D	C.V (%)	Mean	S.D	C.V (%)	Mean	S.D	C.V	Direction
P004/S0020lre (MI)	V1	1.032	.066	6.4	I[a]	I	I	I	I	I	0.356	.036	10.2	U[a]
	V2	1.129	.080	7.1	I	I	I	I	I	I	0.473	.029	6.2	U
	V3	0.012	0	6.3	0.321	.01	6.1	0.969	.06	7.1	0.649	.033	5.2	U
	V4	0.785	.050	6.4	0.591	.033	5.7	0.736	.02	3.2	0.549	.068	12.4	U
P013/s0045lre (MI)	V1	0.766	.024	3.2	I	I	I	I	I	I	0.654	.032	4.9	U
	V2	1.318	.054	4.1	I	I	I	I	I	I	0.254	.018	7.1	U
	V3	0.002	I	I	0.09	.004	5.1	0.85	.05	5.9	0.214	.006	2.9	U
	V4	0.069	.003	4.9	0.39	.020	5.2	0.574	.024	4.3	0.137	.005	3.8	U
P177/s0291lre (normal)	V1	0.005	I	I	0.399	.021	6.3	0.638	.039	6.2	0.025	.001	6.3	In[a]
	V2	0.002	I	I	0.799	.039	4.9	0.301	.009	3.1	0.432	.047	11.1	U
	V3	0.009	I	I	0.776	.055	7.1	1.610	.07	4.9	0.695	.056	8.2	U
	V4	0.003	I	I	1.502	.103	6.9	0.920	.02	2.2	0.722	.06	9.1	U
P104/s0306lre (normal)	V1	0.010	I	I	0.125	.006	4.9	0.973	.07	7.9	0.035	.001	4.2	In
	V2	0.002	I	I	0.371	.013	3.6	1.195	.14	12.2	0.375	.028	7.5	U
	V3	0.003	I	I	0.996	.040	4.1	1.629	.08	5.5	0.341	.017	5.2	U
	V4	0.002	I	I	2.638	.134	5.1	0.785	.01	2.2	0.367	.04	10.9	U

[a] Narration: I: Insignificant measurement, U: Upright, In: Inverted.

Table 5
Comparison with other reported works.

Database	Beat detector	No. of beats	*TP*	*FN*	*FP*	S_e (%)	PP (%)
mit-db	Presented work	19,098	19,022	76	40	99.6	99.5
	Afonso et al. [25]	90,909	90,535	406	374	99.59	99.56
	Bahoura et al. 26]	109,809	109,635	135	184	99.83	99.88
	Lee et al. [27]	109,481	109,146	335	137	99.69	99.88
	Pan and Tomkins [5]	109,809	109,532	277	507	99.75	99.54
	Sahambi et al. [17]	14,481	Not reported	84	93	98.78	Not reported
	Hamilton [28]	Not reported	Not reported	Not reported	Not reported	99.80	99.80
	Arzeno et al. [29]	109,456	107,344	2112	884	98.07	99.59
ptb-db	Presented work	42,852	42,779	73	8	99.84	99.9

facilitates the comparison of the whole data set with the mean. COV is a dimension less number which also gives the measure of dispersion within a series of data. The percentage value shows the dispersion as a percentage of mean. The different time and amplitude features, with mean, SD and COV measures are provided in Table 3 and Table 4 respectively.

Table 5 shows a comparison of the test results of the proposed method with reported works, which use the first channel of mit-db.

4. Discussion

On decomposing the signal till level 10, the last level, *A*10, is observed to have baseline drift as shown in Fig. 2 and Fig. 5C. And the baseline drift correction is done by reconstruction of the signal without *A*10.

The algorithm employs use of some threshold values, for the purpose of peaks, QRS onset and offset detection. These values are empirically set after testing the algorithm on several lead records and calculating the actual possibility of the corresponding limit.

5. Conclusion

The proposed method uses multiresolution feature extraction using DWT, which can be used for feature extraction from ECG data. Additional features like T wave direction, pathological Q, etc. can be used for characterization of the ECG wave. This paper also explores multiresolution analysis for identification of various frequencies present in an ECG signal. The noise frequencies are also identified and eliminated. The proposed method yields a sensitivity of 99.84% and Predictivity of 99.92% with ptb-db. With mit-db files, these figures are 99.6% and 99.5% respectively. Reconstruction scales are selected on the basis of the power spectra of different parts of the signal, which eliminates various noise and artifacts and the interference of other part of the signal while extracting a particular wave or complex. In future an ECG classifier can be proposed, for categorization of various kinds of abnormalities.

References

[1] Leo Schamroth, An Introduction to Electrocardiography, seventh ed., Wiley, India, 2009.

[2] B.U. Kohler, C. Hennig, R. Orglmeister, The principles of software QRS detection, IEEE Eng. Med. Biol. Mag. 21 (1) (2002) 42–57.

[3] C. Saritha, V. Sukanya, Y. Narasimha Murthy, ECG analysis using wavelets, Bulg. J. Phys. 35 (2008) 68–77.

[4] P. Ranjith, ECG analysis using wavelet transform: application to myocardial ischemia detection, ITBM-RBM 24 (January) (2003) 44–47.

[5] J. Pan, W.J. Tomkins, A real time QRS detection algorithm, IEEE Trans. Biomed. Eng. 32 (3) (1985).

[6] O. Pahlm, L. Sörnmo, Software QRS detection in ambulatory monitoring – a review, Med. Biol. Eng. Comput. 22 (July) (1984) 289–297.

[7] F. Gritzali, Toward a generalized scheme for QRS detection in ECG waveforms, Signal Process. 15 (September) (1988) 183–192.

[8] G.M. Friesen, T.C. Jannett, M.A. Jadallah, S.L. Yates, S.R. Quint, H.T. Nagle, A comparison of the noise sensitivity of nine QRS detection algorithms, IEEE Trans. Biomed. Eng. 37 (January) (1990) 85–98.

[9] I. Murthy, G.D. Prasad, Analysis of ECG from pole-zero models, IEEE Trans. Biomed. Eng. 39 (July) (1992) 741–751.

[10] J. Vila, Y. Gang, J. Presedo, M. Fernandez-Delgado, M. Malik, A new approach for TU complex characterization, IEEE Trans. Biomed. Eng. 47 (June) (2000) 764–772.

[11] John Darrington, Towards real time QRS detection: a fast method using minimal pre-processing, Biomed. Signal Process. Control 1 (1) (2006) 169–176.

[12] A.S.M. Koeleman, H.H. Ros, T.J. van den Akker, Beat-to-beat interval measurement in the electrocardiogram, Med. Biol. Eng. Comput. 23 (August) (1985) 213–219.

[13] I.K. Daskalov, I.A. Dotsinsky, I.I. Christov, Developments in ECG acquisition, preprocessing, parameter measurement and recording, IEEE Eng. Med. Biol. Mag. 17 (September) (1998) 50–58.

[14] Nitish V. Thakor, John G. Webster, Wills J. Tompkins, Estimation of QRS complex power spectra for design of a QRS filter, IEEE Trans. Biomed. Eng. 31 (11) (1984).

[15] J.G.C. Kemmelings, A.C. Linnenbank, S.L.C. Muilwijk, A. Sippens-Groenewegen, A. Peper, C.A. Grimbergen, Automatic QRS onsetand offset detection for body surface QRS integral mapping of ventricular tachycardia, IEEE Trans. Biomed. Eng. 41 (September) (1994) 830–836.

[16] C. Li, C. Zheng, C. Tai, Detection of ECG characteristic points using wavelet transforms, IEEE Trans. Biomed. Eng. 42 (January) (1995) 21–28.

[17] J.S. Sahambi, S. Tandon, R.K.P. Bhatt, Using wavelet transform for ECG characterization, IEEE Eng. Med. Biol. 16 (1) (1997) 77–83.

[18] Jerome Dumont, Alfredo I. Hernandez, Guy Carrault, ECG beat delineation with an evolutionary optimization process, IEEE Trans. Biomed. Eng. 57 (3) (2010) 607–615.

[19] Mehmet Engin, ECG beat classification using neuro-fuzzy network, Pattern Recognit. Lett. 25 (15) (2004) 1715–1722.

[20] Themis P. Exarchos et al., Association rule-mining based methodology for automated detection of ischemic ECG beats, IEEE Trans. Biomed. Eng. 53 (8) (2006).

[21] Kang-Ping Lin, Walter H. Chang, QRS feature extraction using linear prediction, IEEE Trans. Biomed. Eng. 36 (10) (1989).

[22] I. Daubechies, The Wavelet Transform, Time-frequency localization and signal analysis, IEEE Trans. Inform. Theory 36 (5) (1990) 961–1005.

[23] PTB Diagnostic ECG database directory, Physiobank Archive Index, PTB Diagnostic ECG database <http://physionet.org/physiobank/daabase>.

[24] Amara Grap, An introduction to wavelets, IEEE Trans. Comput. Sci. Eng. 2 (2) (1995).

[25] V.X. Afonso, W.J. Tompkins, T.Q. Nguyen, S. Luo, ECG beat detection using filter banks, IEEE Trans. Biomed. Eng. 46 (February) (1999) 192–201.
[26] M. Bahoura, M. Hassani, M. Hubin, DSP implementation of wavelet transform for real time ECG wave forms detection and heart rate analysis, Comput. Meth. Prog. Biomed. 52 (2) (1997) 35–44.
[27] J. Lee, K. Jeong, J. Yoon, M. Lee, A simple real-time QRS detection algorithm, in: Proc. 18th Ann. Int. Conf. IEEE Eng. Med. Biol. Soc., vol. 51, no. 2, 1996, pp. 1396–1398.
[28] P. Hamilton, Open source ECG analysis, in: Computers in Cardiology, CA:, IEE, Computer Society Press, Vol.29,no.3, pp. 101–104, March, 2002.
[29] Natalia M. Arzeno, Zhi-De Deng, Chi-Sang Poon, Analysis of first derivative based QRS detection algorithm, IEEE Trans. Biomed. Eng. 55 (2) (2008) 478–484.
[30] A. Ghaffari, H. Golbayani, M. Ghasemi, A new mathematical based QRS detector using continuous wavelet transform, Comput. Electr. Eng. 34 (2) (2008) 81–91.
[31] Physiobank Archive Index, MIT-BIH Arrhythmia Database, <http://www.physionet.org/physiobank/database>.
[32] Abdulnasir Hossen, Bader Al-Ghunaimi, A wavelet-based soft decision technique for screening of patients with congestive heart failure, Biomed. Signal process. Control 2 (May) (2007) 135–143.
[33] Mehmet Engin, Musa Fedakar, Erkan Zeki Engin, Mehmet Korürek, Feature measurements of ECG beats based on statistical classifiers, Measurement 40 (November) (2007) 904–912.
[34] Sung-Nien Yu, Kuan-To Chou, Integration of independent component analysis and neural networks for ECG beat classification, Expert Systems Appl. 34 (February) (2008) 2841–2849.
[35] E.S. Jayachandran, K. Paul Joseph, R. Acharya U, Analysis of myocardial infarction using discrete wavelet transform, J. Med. Syst. 34 (October) (2010) 985–992.